

A Study on Processing and Performance of a 600dpi Master F-theta Lens

Yong-Woo Park*, Seong-Min Moon**, Sung-Ki Lyu**,#

*Department of Convergence Mechanical Engineering, Gyeongsang National University,

**School of Mechanical & Aerospace Engineering, ReCAPT, Gyeongsang National University

600dpi 마스터 에프세타 렌즈 가공 및 성능에 관한 연구

박용우*, 문성민**, 류성기**,#

*경상대학교 대학원 융합기계공학과, **경상대학교 기계항공공학부, 항공연

(Received 24 January 2020; received in revised form 13 March 2020; accepted 21 March 2020)

ABSTRACT

This study examines the processing and performance of an f-theta lens, one of the main components used in laser printer and laser scanning systems. To design an f-theta lens, the optical path of the components of the laser scanning unit f-theta lens, cylinder lens, and collimator lens must be identified. The goal after machining the master f-theta lens is to understand the optical properties, root mean square, and peak to valley.

Key Words : Laser Scanning Unit(레이저 스캐닝 유닛), F-theta Lens(에프세타 렌즈), Optic(광학), Root Mean Square(표면조도), Peak to Valley(표면형상정도)

1. Introduction

Laser scanning systems in laser compositors and printers serve to convert digital data into light-based information as the computer's digital signal is transmitted to the Laser Scanning Unit. The LSU core components consist of the f-theta scan lens, polygon mirror, cylinder lens, collimator lens, laser diode, laser-controlled circuit board, and case,

among others. The most important core technology in LSU transmits light dots from laser diodes to the drums through the correct light source. Collimator lenses are used to block the scattering of diffuse beams from laser diodes and transform them into parallel beams. The principle here is that the parallel beam from the collimator lens is collected in the direction of vertical scanning to allow the beam from the cylinder lens to form imagery on the face of the polygon mirror; then, the beam is diffused again and entered into the f-theta scan lens.

The f-theta scanning lens is so called because it represents the width of spreading the beam to the

Corresponding Author : sklyu@gnu.ac.kr

Tel: +82-55-772-1632, Fax: +82-55-772-1578

drum by the polygon mirror angle and the tangent value of the focal length f . This f -theta scan lens is one of the LSU most important parts, and significant research has been conducted on it. For instance, Noh et al. has conducted a study on system design for Laser Scanning Units using A3⁽¹⁾, Yoo et al. has conducted a study on the injection molding of a Laser Scanning Unit optical system⁽²⁾, Robert et al. has conducted a study on optical scanning⁽³⁾ and Park et al. has conducted a numerical analysis of the injection molding of an Aspheric lens for a photo pick-up device.⁽⁴⁾ A number of other researchers are conducting additional studies to improve the performance and characteristics of the f -theta scan lens⁽⁵⁻⁹⁾. In this study, the processing and performance of a master f -theta scan lens were evaluated as a prior stage of injection process for the mass production of f -theta scan lenses.

2. Optical Design

2.1 Optical Design of Laser Scanning Unit

Fig. 1 presents the LSU system configuration. The data passed through the LSU is polarized into a corona discharge phenomenon on the surface of the prganic photo conductor drum combined with the toner polarity. This is a structural diagram of how the LSU optical data is transmitted via the principle that data such as letters and pictures are printed by the heating roller as toner is deposited by a polarity attraction force on the paper.

Table 1 presents basic specifications for LSU design. The LSU optical system consists of parts such as the f -theta scan lens, cylinder lens, collimator lens, polygon mirror, and laser diode.

A preliminary study of the optical system simulation was conducted with Code-V, an optical design software, to simulate whether the beam from the laser diode would actually pass through each

lens and emerge beam-sized on the imagery surface. After determining the f -theta scan lens part where the beams pass through at each location, we were able to identify problems in certain areas of the f -theta scan lens. Through these simulation processes, we calculated the values of K is 467.5639, A is -1.44508e-0.7, B is -5.51473e-12, C is 3.51711e-14, and D is -9.93642e-18 with the optical design of the aspherical surface lens of equations (1) and (2).

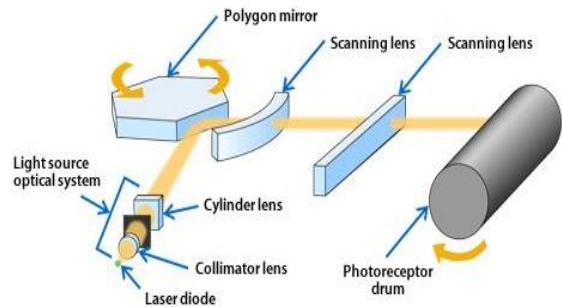


Fig. 1 Laser scanning unit system

Table 1 Specification of laser scanning unit

No.		Spec.
Resolution		600 dpi
Beam size	Main beam	80 +15/-10 μm
	Sub beam	85 +20/-10 μm
LD.	Wave length	785 +10/-15 μm
	Power	0.3±0.02 mW
F-theta lens	Mag. error	Max. 0.7 %
	Part mag. error	Max. 1.5 %
Pitch error	Near	Max. 10 μm
	All	Max. 20 μm
Jitter	Lf	Max. 0.025 %
	Rf	Max. 0.012 %
Scan line property	Bow	Max. 1 mm
	Skew	Max. 1 mm
Polygon motor	Voltage	24V DC±10 %
	Driving method	PWM
	Rotation speed	30,000 rpm
	Mirror thk.	2 mm
	Mirror size	12.99±0.05 mm

$$F(H) = \frac{(CURV1)H^2}{1+(1-(1K)(CURV^2H^2))^{1/2}} \quad (1)$$

$$+ (A)H^4 + (B)H^6 + (C)H^8 + (D)H^{10}$$

$$Z = F(H) + (1/2) * CURV2 * (S^2 + Z^2 - F^2(H))$$

$$Z = \frac{(CURV)Y^2}{1+(1-(1+K)(CURV^2Y^2))^{1/2}} \quad (2)$$

$$+ (A)Y^4 + (B)Y^6 + (C)Y^8 + (D)Y^{10}$$

$$Z = \frac{Y^2}{R1[1 + \sqrt{1 - (1+1K1)(1/R1)^2 Y^2}]} \quad (3)$$

$$+ A1Y^4 + B1Y^6 + C1Y^8 + D1Y^{10}$$

2.2 Optical Design of F-theta Lens

An important element in LSU optical system design is the enhancement of light-gathering power to achieve high resolution and high resolving power. Additionally, the use of various lens materials, the degree of design freedom, and the ease of machining due to high processing characteristics should be considered. Taking these factors into account, the optical design of the f-theta lens was carried out based on the optical system design and simulation data.

In this study, we used a master f-theta lens featuring one free curve and a aspherical surface. Table 3 presents the specifications of this f-theta lens. Equation (3) is the aspherical optical design of the F-theta lens. R1Y represents the plane of incidence, is Y toric, R1 is -1195.109605323, K is 467.5639421656, A1 is -1.445075408806e-007, B1 is 5.514734404114e-012, C1 is 3.51811117087e-014, and D1 -9.936422767774e-018.

Meanwhile, R2Y represents the plane of projection, is X toric, R2Y is -70.6551685798, and R2X is -18.06639282.

The f-theta lens optical system was designed as presented in Fig. 2 with Code-V, an optical design software. Table 4 shows the optical design value for the effective plane of the f-theta lens.

Table 3 Specification of f-theta lens

No.		Spec.
Effective scan width		A3(297 mm)
Lens number		1 Pcs
Focal Length		A3 type 210 mm
Polygon mirror		φ 30 mm, 6 facets
Beam dia.	Main	75 μm(+15/-10) ↓
	Sub	80 μm(+20/-10) ↓
Laser wavelength		785 nm(+15/-10)
Ambient Light Ratio		80 % ↑
Magnification error		0.7 % ↓
Partial magnification error		1.5 % ↓

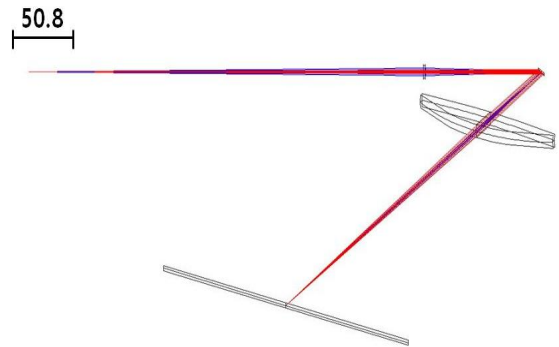


Fig. 2 2D Lay out of f-theta lens using Code-V

Table 4 Effective surface optical of the f-theta lens

Part	R1	R2
Rad.	119.5.110 CC	70.655 CX
Rad. tol	±0.025	±0.025
Pow./Irr.	5.0/1.0	5.0/1.0
C.A.D	80	96
Edge dia.	100.19	
Dia. tol.	0.	
Thi.	22	
Thi. tol.	±0.025	
Wedge	±0.025 T.L.R	

3. Lens Machining

To process the master f-theta lens based on the optical data designed, 2D drawings were produced with the AutoCAD design software (as Fig. 3 shows). To carry out shape machining, 3D modeling was performed with the CATIA V5 design software (as Fig. 4 shows). Based on the completed modeling data, the high-speed processing machine (Makino V56) was used for initial processing to perform rough machining; this is presented in Fig. 5. For the secondary processing, we used the DTM (Diamond Turning Machine: Toshiba, UNC-100F), an ultra-precision processing tool. Moreover, we used special bites for master f-theta lens processing to perform finished cutting machining (as Fig. 6 shows). Finally, Fig. 7 presents the master f-theta lens that was machined via the repetition process of rough machining and finished cutting machining.

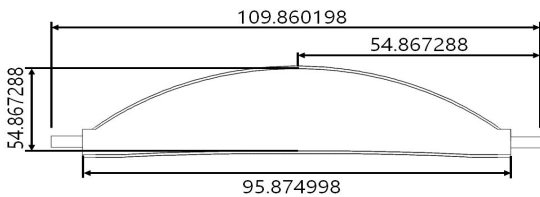


Fig. 3 2D Design of the f-theta lens using AutoCAD

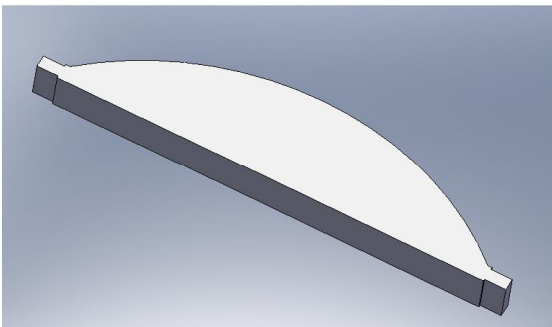


Fig. 4 3D Modeling of the f-theta lens using CATIA V5

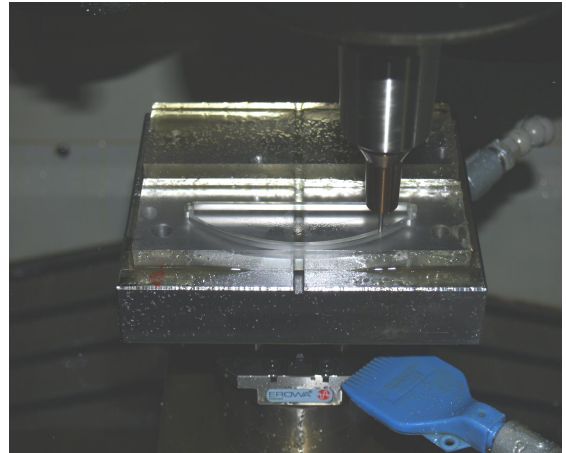


Fig. 5 Roughing process of master f-theta lens



Fig. 6 Finishing process of master f-theta lens



Fig. 7 Master f-theta lens

4. Experiments and Reviews

The root mean square and peak to valley of the machined master f-theta lens were measured with UA3P (UA3P: Panasonic 3D profilometer), an ultra-precision measuring tool. The measurement criteria were based on the values that satisfy the root mean square of $0.06\mu\text{m}$ and the peak to valley of $0.3\mu\text{m}$ or less; in other words, the measurement criteria for aspherical lenses. As Fig. 8 shows, the results of the first processing measurements that were more unstable than the reference value exhibited the values of, respectively, $8.7735\mu\text{m}$ in the plane of incidence root mean square, $33.6959\mu\text{m}$ in peak to valley, $24.0747\mu\text{m}$ in the plane of projection root mean square, and $83.8028\mu\text{m}$ in peak to valley. Subsequently, the bites used for rough machining and finished cutting machining were modified and re-manufactured before proceeding with re-processing. The measurements taken after the secondary machining satisfied the reference values; these measurements were $0.0362\mu\text{m}$ for plane of incidence peak to valley, $0.1955\mu\text{m}$ for peak to valley, $0.0442\mu\text{m}$ for plane of projection root mean square, and $0.2133\mu\text{m}$ for surface shape precision (as Fig. 9 shows).

In order to identify problems caused by the machining process rather than the injection process, the homogenous condition inside the master f-theta lens with completed processing was checked using polaroid film. Fig. 10 shows the double refraction condition inside the lens immediately after processing it. The lens' fogginess (such as the fog inside the lens) is caused by the presence of fine bubbles; thus, the refraction of the beam transmitted to the f-theta lens is not smooth and incapable of ensuring adequate performance. Therefore, as a result of heat-based calibration, the double refraction condition confirmed good improvement in the double refraction shape (as Fig. 11 shows). The master f-theta lens was demonstrated to satisfy

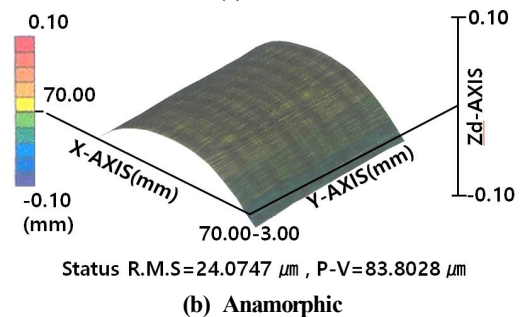
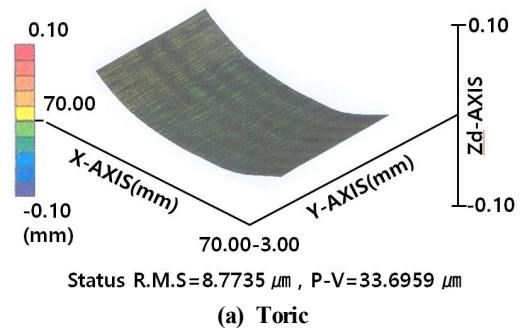


Fig. 8 1st result RMS & P-V of master f-theta lens using UA3P

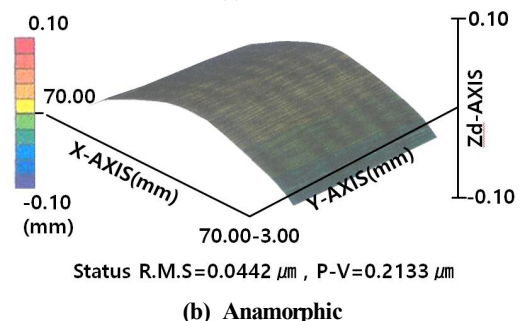
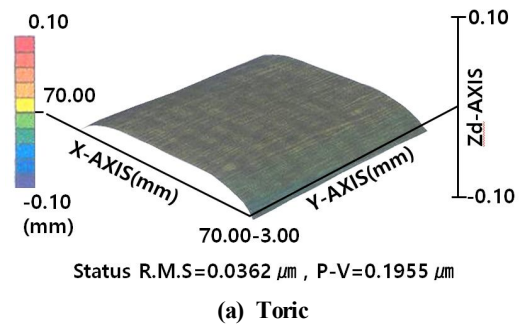


Fig. 9 2nd result RMS & P-V of master f-theta lens using UA3P

both values of the root mean square and peak to valley in the plane of incidence, plane of projection required as aspherical lenses. These results are illustrated in Fig. 12.

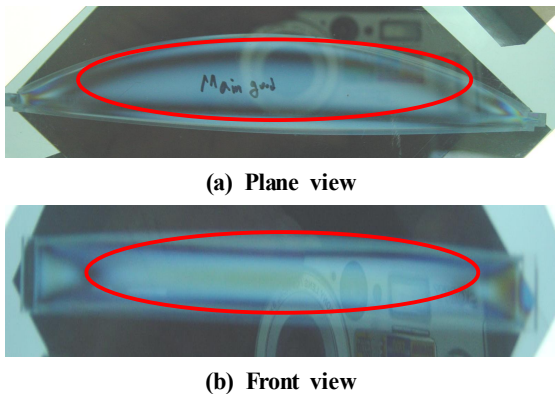


Fig. 10 1st result double refraction view of master f-theta lens

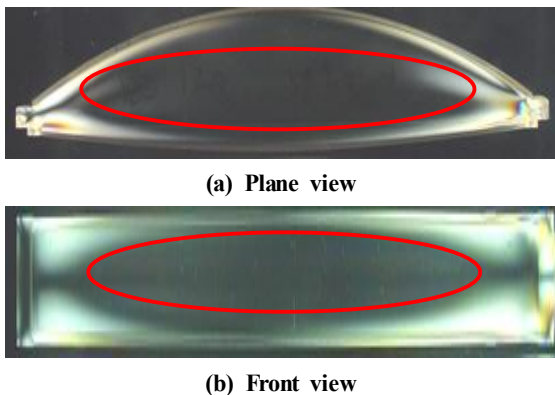


Fig. 11 2st result double refraction view of master f-theta lens



Fig. 12 Master f-theta lens

5. Conclusion

This study confirmed the optical performance of a master f-theta lens for the significant surface through precision high-speed processing and ultra-precision processing of a Laser Scanning Unit 600 dpi master f-theta lens. We believe that the study's data will enable significant performance improvement and mass production of f-theta lens optics in the future. Below, the study's main findings are summarized.

- (1) The plane of incidence root mean square of the master f-theta lens was found to be $0.0362 \mu\text{m}$ while the peak to valley was $0.1955 \mu\text{m}$. Thus, the reference values of aspherical lenses; the root mean square of $0.06 \mu\text{m}$ and the peak to valley of $0.3 \mu\text{m}$ or less, were all satisfied.
- (2) The plane of projection root mean square of the master f-theta lens was found to be $0.0442 \mu\text{m}$ while the peak to valley was $0.2133 \mu\text{m}$. Both the peak to valley of the aspherical lens (the reference value of $0.06 \mu\text{m}$) and the peak to valley (within the reference value of $0.3 \mu\text{m}$) were satisfied.
- (3) This study effectively confirmed that the double refraction shape of the master f-theta lens can be improved via heat-based calibration.

ACKNOWLEDGEMENT

This study was supported by the Basic Science Research Program through the NRF of Korea (NRF) funded by the MEST(NRF-2020R1A2C1011958).

REFERENCES

1. Noh, M. J., Hyun, D. H., Chang, H. S., Park, Y.

- W., and Park, C. Y., "System Design for Laser Scanning Unit using A3", Journal of the Korean Society of Manufacturing Technology Engineers, Vol. 11, No. 4, pp. 71-72, 2011.
2. Yoo, K. S., Hyun, D. H., Chang, H. S., Park, Y. W. and Park, C. Y., "Injection Molding of a Laser Scanning Unit Optical System", Journal of the Korean Society of Manufacturing Technology Engineers, Vol. 11, No. 4, pp. 102-103, 2011.
 3. Robert, E. Hopkins and David Stephenson, Optical Scanning(Marcel Dekker), pp. 27~82, 1991.
 4. Park, K., and Han, C. Y., "Numerical Analysis for the Injection Molding of an Aspheric Lens for a Photo Pick-up Device", Journal of the Korean Society of Precision Engineering, Vol. 21, No. 11, pp. 163~170, 2004.
 5. Lee, D. K., Yang, Y. S, Kim,, S. S., Kim, H. J., and Kim, J. H, "Development of F theta Lens for Laser Scanning Unit", Journal of the Korean Physical Society, Vol. 53, Issue 915, pp. 2527, 2008.
 6. Rim, C. S., "The effect analysis of birefringence of plastic f-theta lens on the beam diameter", Korean Journal of the Optics and Photonics, Vol. 10, No. 1, pp. 15-20, 1999.
 7. Bringans, R. D., "Application of Blue Diode Lasers to Printing," Proc. of Materials Research Society Symposium, Vol. 482, pp. 1203-1210, 1998.
 8. Sakuma, N., "Aspherical Surface in the Laser Writing Optics", Optical Design, No. 17, pp. 9-15, 1999.
 9. Kazuo, M., "Historical review and Future Trends of Scanning Optical Systems for Laser Beam Printers", Electronic imaging device engineering Proceedings, Vol. 1987, pp. 21-25, 1993.